

Chapter 5

Vegetation Cover in the Eurasian Arctic: Distribution, Monitoring, and Role in Carbon Cycling

Olga N. Krankina, Dirk Pflugmacher, Daniel J. Hayes, A. David McGuire, Matthew C. Hansen, Tuomas Häme, Vladimir Elsakov, and Peder Nelson

Abstract Comparison of several recent, publicly available and widely used land-cover products for the Eurasian Arctic revealed important differences in their representations of vegetation distribution. Such disparities have important implications for models that use these products as driving data sets to monitor vegetation and its role in carbon dynamics. The differences between GLC-2000 and MODIS.PFT are concentrated at borders between biomes, as well as in parts of the region where a significant presence of open-canopy vegetation is expected. In these two maps, tree cover is represented more consistently than shrub or herbaceous cover, and the MODIS.VCF product corroborates the general pattern of tree-cover distribution. The comparison of the MODIS.VCF and AVHRR.VCF maps over northeastern Europe indicates good agreement in the south with increasing disagreement further north primarily due to differences in definitions of the mapped variables. The analysis of land-cover maps at two Landsat validation sites showed different patterns of agreement and disagreement. At the forest dominated St. Petersburg site, the GLC-2000 and MODIS.PFT classifications both exaggerated tree cover and under-reported shrub and herbaceous vegetation. At the tundra site (Komi), the over-reporting of tree cover by GLC-2000 and the failure of MODIS.PFT to separate shrub and herbaceous vegetation were the major issues in representing the overall land cover. A simple analysis that extrapolated results of biogeochemical modeling showed that a very different picture of the regional carbon balance emerges when different vegetation maps are used as model inputs.

5.1 Introduction

Accurate mapping of land cover and monitoring its change are fundamental requirements for global change research. These are especially important in the Arctic zone, which has experienced rapid rates of warming in recent years and the evidence of

O.N. Krankina (✉)
Department of Forest Ecosystems and Society, Oregon State University, Corvallis,
OR 97331, USA
e-mail: krankinao@fsl.orst.edu

regional impacts of warmer climate is mounting (Anisimov et al. 2007). Vegetation cover is expected to generate potentially critical, but not fully understood, feedbacks to a changing climate as a function of surface energy balance and the patterns of sources and sinks of atmospheric carbon dioxide (CO₂) and other greenhouse gases (Chapin et al. 2005; Field et al. 2007; Houghton 2003). In addition to direct climate forcings, natural disturbances and human activities can substantially alter the patterns and processes that create and transform these terrestrial sources and sinks (Houghton et al. 2004; Schimel et al. 2001).

The terrestrial ecosystems of the Arctic cover approximately 25% of the Earth's vegetated land surface (McGuire et al. 1997) and contain about one third of the total global terrestrial ecosystem carbon (C) pool (Schlesinger 1991). The large land area of boreal and arctic ecosystems across Northern Eurasia represents a key component in both the high latitude and global C budgets. In recent decades, this region has experienced extensive and severe forest fires (Sukhinin et al. 2004), along with changes in land use and forest management (Krankina et al. 2005). Studies using various accounting and modeling approaches, including top-down atmospheric inversions (Gurney et al. 2004) and bottom-up inventory-based estimates (Shvidenko and Nilsson 2003; Myneni et al. 2001) have suggested a positive terrestrial C balance (terrestrial sink) in Northern Eurasia during recent decades. More recent process-based model estimates by Balshi et al. (2007), which include the 2002 fire year, suggest that the large area burned may be causing the region to shift toward a net CO₂ source to the atmosphere. The combined effects of the recent changes in climate (Polyakov et al. 2002), disturbance (Sukhinin et al. 2004) and land management (Krankina et al. 2005) on the contemporary C budget of this region are examined in [Chapter 6](#), this volume.

The models that are being used to investigate the role of arctic vegetation in the global climate system require complete coverage with accurate and repeated measures of vegetation and land cover attributes as key driving variables. Several moderate and coarse resolution land-cover datasets are available for the Eurasian Arctic region (Hansen et al. 2000; Loveland et al. 2000; Friedl et al. 2002; Bartalev et al. 2003; Fritz et al. 2003; Hansen et al. 2003a, b), and more are being developed. However, there is a significant disagreement among these datasets and high latitudes appear particularly problematic for land-cover mapping (Giri et al. 2005; Fritz and Lee 2005; Herold et al. 2008; Krankina et al. 2008). This is not surprising because all of these datasets rely on spectral satellite imagery. The high level of cloudiness, in combination with low sun angle and the shortness of the growing season in the Arctic, reduces data availability from passive sensors.

The accuracy of land-cover products for Arctic regions and the product utility for various applications remains largely uncertain. This is because the validation of coarse resolution maps is a persistent challenge, particularly for Northern Eurasia where validation sites are sparse, several land-cover types are unique, and processes of ecosystem disturbance and land-cover change are widespread, including fire, timber harvest, insect outbreaks, agricultural conversion and abandonment, forest regrowth, and melting permafrost. The lack of independent validation makes it often impossible to ascertain which products perform better in specific geographic

domains, for specific land-cover types, or in specific applications. Detailed examination of available global land-cover products showed that the classification legends are not well suited for parameterizations of C cycling models, which is among the major applications of global and continental land-cover maps (Jung et al. 2006).

Changes in land cover are among the principal indicators of the impact of global change on terrestrial ecosystems. While some aspects of Earth surface cover (e.g., sea ice) have been carefully monitored and, in fact, show significant change (e.g., Stroeve et al. 2006), change in land cover has not received the same level of attention (see review of recent studies in Chapter 2 by Goetz et al., this volume). The shortness of the satellite data record relative to the temporal scale of vegetation succession is an inherent difficulty in monitoring vegetation change and this problem is particularly significant in the Arctic. At present, coarse resolution sensors such as MODIS are investigated for their potential to track many forms of vegetation change. The MODIS record is now long enough to support monitoring of forest ecosystem disturbance and recovery (Hansen et al. 2010; Potapov et al. 2008; Chapter 3, this volume). In the future, the growing length of the data record will further expand opportunities for monitoring land-cover change. However, the disagreement among the maps of current vegetation cover results in uncertainty as to which land-cover type undergoes change and indicating an urgent need for improved land-cover mapping.

This study examines recent, publicly available and widely used land-cover products representing two principal approaches to mapping vegetation cover in the Eurasian Arctic: categorical maps and continuous field maps. First, we cross-compare the regional datasets and then we validate them in two locations using detailed, Landsat-based maps derived from local ground data and knowledge of land cover. Finally, we assess the significance of the current uncertainty in vegetation cover for estimating C stores, sources and sinks in terrestrial ecosystems of the region and outline approaches for improved regional representation of land cover.

5.2 Representation of Vegetation Cover in Coarse Resolution Maps

Knowledge about the distribution and dynamics of arctic vegetation has improved in the last two decades through the development of coarse resolution satellite-based land-cover maps. The first global land-cover map based on remote sensing was developed by DeFries and Townshend (1994) with data from the Advanced Very High Resolution Radiometer (AVHRR) sensor at one-degree spatial resolution. Later, maps with finer resolution (1-km) were developed using AVHRR data acquired between April 1992 and March 1993: the Global Land Cover Characterization (GLCC) data base (Loveland et al. 2000) and the University of Maryland (UMD) Global Land Cover (GLC) data set (Hansen et al. 2000). Although the two maps utilized the same sensor data, the mapping methodologies differed

considerably, which led to disagreements between the two maps (Hansen et al. 2000). In addition to land-cover maps based on satellite observations, regional maps are also produced based on legacy geobotanical data sets with remotely sensed data used primarily for georeferencing of polygons that represent various landscape types and delineating areas of high shrub within some provinces (Walker et al. 2005). Because of the large size of polygons on geobotanical maps a direct comparison with satellite-based land-cover products appears problematic.

5.2.1 Comparison of Categorical Maps

The two major recent global land-cover mapping activities are the Global Land Cover 2000 (GLC-2000) (Fritz et al. 2003) and the Moderate Resolution Imaging Spectroradiometer (MODIS) land-cover product (Friedl et al. 2002). The GLC-2000 mapping was lead by the Joint Research Center of the European Commission in partnership with more than 30 institutions around the world (Fritz et al. 2003), and MODIS land cover product was prepared by scientists from Boston University for US National Aeronautics and Space Administration's (NASA) Earth Observing System (EOS) MODIS land science team (Friedl et al. 2002). The two maps have a 1-km spatial resolution, but they were created using different satellite data, methodologies and classification schemes. For example, the global GLC-2000 map was derived from 19 regional subsets with regionally specific classification schemes. In comparison, the MODIS team used a global classification approach involving training sites distributed across the globe.

We assessed the agreement between these two maps, GLC-2000 and MODIS land cover, in representing the Dominant Vegetation Types (DVTs) which we defined as trees, shrubs, herbaceous vegetation, and barren with sparse vegetation. MODIS land cover (MOD12Q1) is available in five classification schemes (IGBP, UMD, LAI/fPAR, BGC and PFT). We obtained the PFT (Plant Functional Types) layer for Eurasia for the year 2001 (V004) in Lambert Azimuthal Equal-area (LAEA) projection (<http://duckwater.bu.edu/lc/mod12q1.html>; last accessed 20 February 2008). The MODIS.PFT classification consists of 12 classes and was developed for the National Center for Atmospheric Research (NCAR) land surface model (Bonan et al. 2002).

The GLC-2000 map is based on Satellite Pour l'Observation de la Terre (SPOT) VEGETATION data acquired daily between November 1999 and December 2000. The GLC-2000 uses a legend based on the hierarchical Land Cover Classification System (LCCS, Di Gregorio 2005). Both, the regional products (e.g., Bartalev et al. 2003 for Northern Eurasia) and a global mosaic of the regional products with a harmonized legend are available. We downloaded the global data set (v1.1) from (<http://www-gvm.jrc.it/glc2000/>; last accessed 20 January 2008) in geographic coordinate space, and reprojected it to LAEA, the geographic reference system of the MODIS map.

To assess the spatial agreement between GLC-2000 and MODIS.PFT, we cross-referenced the LCCS and PFT legends using the DVT logic (Table 5.1). While

Table 5.1 Agreement/disagreement matrix for GLC-2000 and MODIS.PFT land cover

	1	2	3	4	5	6	7	8	9	10	11	0
	Needleleaf evergreen tree	Broadleaf evergreen tree	Needleleaf deciduous tree	Broadleaf deciduous tree	Shrub	Grass	Cereal crop	Broadleaf crop	Urban and built-up	Snow and ice	Barren or sparsely vegetated	Water
GLC-2000.LCCS (rows) MODIS.PFT (columns)												
1 Tree cover, broadleaved, evergreen	T	T	T	T	ts	th	th	th	tb	tb	tb	lw
2 Tree cover, broadleaved, deciduous, closed	T	T	T	T	ts	th	th	th	tb	tb	tb	lw
3 Tree cover, broadleaved, deciduous, open	T	T	T	T	ts	th	th	th	tb	tb	tb	lw
4 Tree cover, needle-leaved, evergreen	T	T	T	T	ts	th	th	th	tb	tb	tb	lw
5 Tree cover, needle-leaved, deciduous	T	T	T	T	ts	th	th	th	tb	tb	tb	lw
6 Tree cover, mixed leaf type	T	T	T	T	ts	th	th	th	tb	tb	tb	lw
7 Tree cover, regularly flooded, fresh water	T	T	T	T	ts	th	th	th	tb	tb	tb	lw
8 Tree cover, regularly flooded, saline water	T	T	T	T	ts	th	th	th	tb	tb	tb	lw
9 Mosaic: Tree cover/other natural vegetation	T	T	T	T	S	H	th	th	tb	tb	tb	lw
10 Tree cover, burnt	T	T	T	T	ts	th	th	th	tb	tb	tb	lw
11 Shrub cover, closed-open, evergreen	ts	ts	ts	ts	S	sh	sh	sh	sb	sb	sb	lw
12 Shrub cover, closed-open, deciduous	ts	ts	ts	ts	S	sh	sh	sh	sb	sb	sb	lw
13 Herbaceous cover, closed-open	th	th	th	th	sh	H	H	H	hb	hb	hb	lw
14 Sparse herbaceous or sparse shrub cover	tb	tb	tb	tb	sb	hb	hb	hb	B	B	B	lw
15 Regularly flooded shrub and/or herbaceous cover	ts	ts	ts	ts	S	H	H	H	hb	hb	hb	lw
16 Cultivated and managed areas	th	th	th	th	sh	H	H	H	hb	hb	hb	lw
17 Mosaic: cropland / Tree cover / other natural vegetation	T	T	T	T	S	H	H	H	hb	hb	hb	lw
18 Mosaic: cropland / shrub and/or herbaceous cover	th	th	th	th	S	H	H	H	hb	hb	hb	lw
19 Bare areas	tb	tb	tb	tb	sb	hb	hb	hb	B	B	B	W
20 Water bodies (natural & artificial)	lw	lw	lw	lw	lw	lw	lw	lw	lw	lw	lw	W
21 Snow and ice (natural & artificial)	tb	tb	tb	tb	sb	hb	hb	hb	B	B	B	lw
22 Artificial surfaces and associated areas	tb	tb	tb	tb	sb	hb	hb	hb	B	B	B	lw

Agreement: T = tree, S = shrub, H = herbaceous, B = barren/sparse vegetation, W = water; Disagreement: ts = tree-shrub, th = tree-herbaceous, tb = tree-barren, sh = shrub-herbaceous, sb = shrub-barren, hb = herbaceous-barren, lw = land-water

the MODIS.PFT classification translates directly into the four DVT classes, the GLC-2000 classification featured four out of 22 classes with no unique dominant vegetation type (three mosaic classes and a “regularly flooded shrub and/or herbaceous cover” class; Table 5.1). In these four cases multiple types of agreement were possible. For example, if GLC-2000 mapped a pixel as “Mosaic: Cropland, Tree cover and other natural vegetation,” this pixel was considered in agreement with MODIS tree, shrub or herbaceous classes, but in disagreement with MODIS barren and sparsely vegetated classes (including “Urban and built-up”, “Snow and ice” and “water”). Land cover mosaics and “regularly flooded shrub and/or herbaceous cover” class occupy $330 \times 10^3 \text{ km}^2$ (3.7%) and $688 \times 10^3 \text{ km}^2$ (7.6%), respectively, on GLC-2000 map.

The comparison of the GLC-2000 and MODIS.PFT land-cover maps showed significant differences between the two maps in representing dominant vegetation types, mainly tree and shrub vegetation. According to GLC-2000, 50% of the Eurasian land area between 60° and 74° N fall into tree dominated vegetation types, followed by 26% shrub types, 14% barren or sparse vegetation and 10% herbaceous vegetation. These percentages include the area of land cover mosaics and regularly flooded shrub and/or herbaceous vegetation, which we assigned to a DVT class after cross-referencing and overlaying the MODIS.PFT map (Table 5.1). In comparison, MODIS.PFT mapped only 30% of the area as tree-dominated, while the majority (60%) was identified as shrub-dominated vegetation types. The MODIS.PFT estimate of herbaceous vegetation cover was similar (8%), but the area defined as barren/sparse vegetation was much smaller than on GLC-2000 map (3%).

The overall spatial agreement between GLC-2000 and MODIS.PFT on a pixel-by-pixel basis was fairly low at 53% (Table 5.2, Fig. 5.1). Most of the disagreement occurred between tree and shrub vegetation (21% of land area), the majority of which is in regions where MODIS.PFT mapped shrub and GLC-2000 mapped tree vegetation (19% of land area). This area of disagreement is consistent with the overall higher representation of tree-dominated cover in the GLC-2000 map (20% higher than MODIS.PFT). In comparison, the 30% of the land area that are mapped as tree vegetation by MODIS.PFT are in good agreement with the GLC-2000 map (91% agreement, Table 5.2). The confusion between GLC-2000 tree and MODIS.PFT shrub vegetation marks the transition zone from boreal forest to shrub tundra and is mostly concentrated on permafrost lands in northeastern Siberia and parts of the Far East (Fig. 5.1) where low-stature open-canopy trees can be difficult to distinguish from shrubs. The second most common disagreement is between MODIS shrub and GLC-2000 barren (11%) and herbaceous vegetation (8%) and it is concentrated primarily in the tundra zone. While 85% of the shrub pixels in the GLC-2000 map were confirmed by MODIS.PFT, only 36% of the pixels identified as shrub by MODIS.PFT were confirmed by GLC-2000 (Table 5.2). The fact that the vegetation types that are mapped conservatively on one map have high level of agreement with the other map (e.g., trees on MODIS.PFT and shrub on GLC-2000) suggests that the mapping results are robust in these cases. Large areas of agreement are concentrated in the western part of the Eurasian Arctic where the availability of ground data for training the mapping algorithms is better (Fig. 5.1).

Table 5.2 Area of agreement and disagreement (in 1,000 km²) for GLC-2000 and MODIS.PFT dominant vegetation types in the Eurasian Arctic (excluding water)

GLC-2000	MODIS.PFT					Agreement (%)
	Tree	Shrub	Herbaceous	Barren	Total	
Tree	2.395	1.697	351	7	4.450	54
Shrub	200	1.922	105	31	2.258	85
Herbaceous	24	698	160	34	916	17
Barren	12	973	64	183	1.232	15
Total	2.630	5.290	680	255	8.855	
Agreement (%)	91	36	23	72		53

Herbaceous vegetation appears to be the most problematic type for finding agreement between the two maps. Even though the total area estimates for herbaceous vegetation are not dramatically different in the two maps, the spatial agreement is very low (<25%, Table 5.2). The confusion of herbaceous vegetation with other vegetation types may stem from the fact that in the Arctic many areas with herbaceous vegetation are in fact wetlands, often with significant presence of *Sphagnum* spp. and other mosses and lichens. This vegetation type has a substantially different spectral reflectance compared to vascular herbaceous plants (Vogelman and Moss 1993; Bubier et al. 1997; Krankina et al. 2008). The test of available global and regional wetland and peatland datasets against detailed land-cover maps for the St. Petersburg region showed that peatlands were correctly classified as such in coarse-resolution datasets but a large proportion (74–99%) was overlooked (Krankina et al. 2008). The under-reporting of the actual extent of wetlands on this scale is especially problematic for estimating carbon stores and flux in the Arctic (McGuire et al. 2007). Even though the potential of MODIS to capture the distribution of boreal wetlands was demonstrated (Pflugmacher et al. 2007), this potential has not been exploited for improving wetland mapping across the Eurasian Arctic and the inconsistent representation of herbaceous vegetation on continental maps may be in part attributable to that.

5.2.2 Vegetation Continuous Field Maps

Unlike categorical maps, Vegetation Continuous Field (VCF) maps provide sub-pixel proportional estimates of land cover. Continuously varying maps of cover provide improved spatial detail when compared to categorical maps that by definition discretize landscapes. Areas undergoing disturbance are more accurately characterized at sub-pixel scales, resulting in map products that more fully exploit the inherent variability found in imagery (Hansen et al. 2002). Unlike classifications, continuous cover maps enable users to define their own thresholds for land-cover classes and can also be used consecutively to identify areas undergoing land-cover change. VCF maps for forest cover have been developed for different regions in

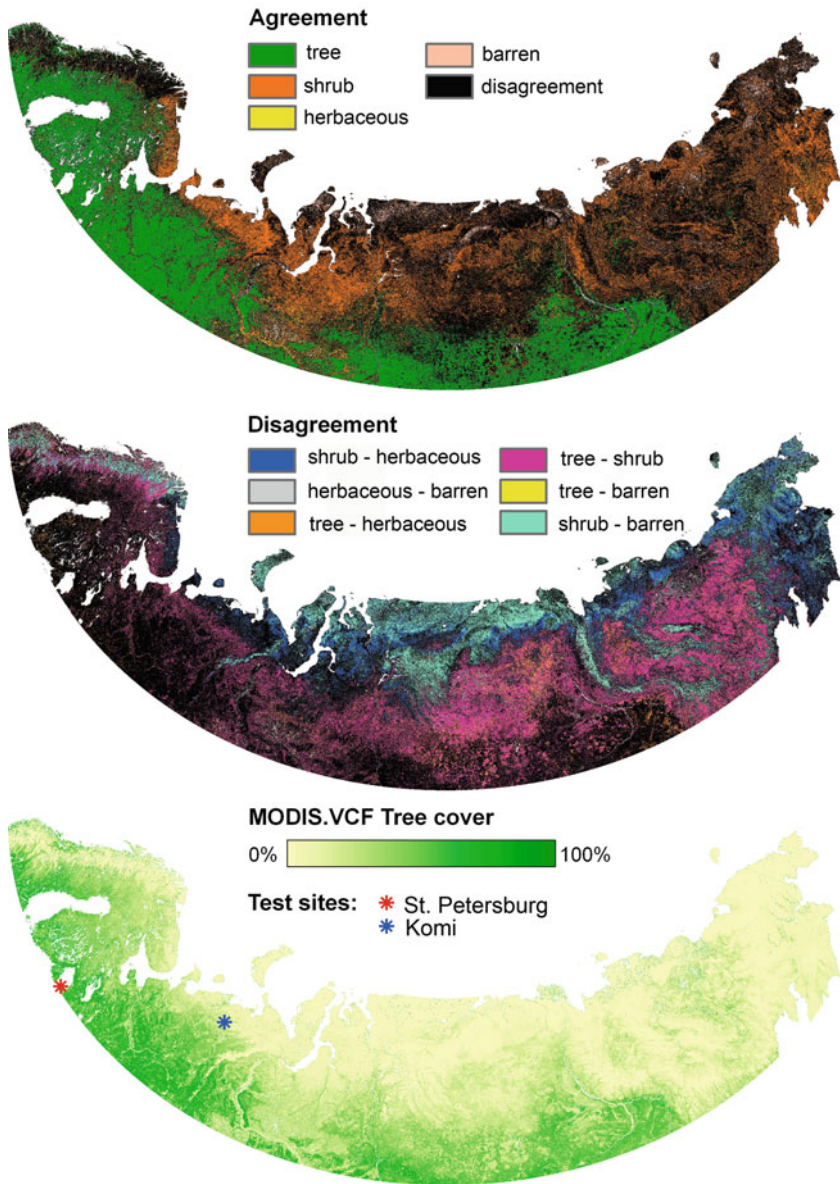


Fig. 5.1 (Top) Maps agreement and (middle) disagreement in dominant vegetation cover for GLC-2000 and MODIS.PFT, and (bottom) MODIS.VCF tree-cover map in the Eurasian Arctic

the world and from different sensor types, e.g., AVHRR (Zhu and Evans 1994; DeFries et al. 1997; Häme et al. 2000 and 2001) and MODIS (Hansen et al. 2005). In this study, we analyze a MODIS-based VCF product for Northern Eurasia and an AVHRR-based VCF product for the pan-European region.

The MODIS.VCF tree canopy cover data set was developed by MODIS land science team members from the University of Maryland at a spatial resolution of 500 m (Hansen et al. 2003a, b). The MODIS.VCF of tree-cover estimates sub-pixel percent tree-canopy cover for the entire globe. Percent tree-canopy cover refers to the amount of skylight orthogonal to the surface that is obstructed by tree canopies equal to or greater than 5 m in height and is different than percent crown cover, which includes both the canopy cover and the within-crown skylight/gaps. Current VCF percent tree-cover products are generated using sub-pixel training data derived from Landsat imagery. Each Landsat pixel is classified as one of four tree-cover strata and assigned a mean canopy-cover value. These values are then averaged to MODIS scale (500 m) and used as reference training data. The training labels are related to annual metrics (Hansen et al. 2002) that are generated from 32-day composites of Terra MODIS data. MODIS bands 1–7, derived Normalized Difference Vegetation Index and Land Surface Temperature are used as inputs (Wolfe et al. 1998; Wan et al. 2002). Annual metrics are time-integrated means, amplitudes, and ranks of annual composite imagery that represent salient features of vegetation phenology without reference to specific time of year, and have been shown to perform as well or better than time-sequential composites in mapping large areas (Hansen et al. 2005). A regression-tree bagging algorithm (Breiman 1996) is used to relate the percent tree-canopy cover training data to the annual metrics in creating the VCF tree-cover product.

Annual VCF tree-cover products are available for 2000–2005 and free for download through the Land Processes Distributed Active Archive Center (<http://edcdaac.usgs.gov>) and through the Global Land Cover Facility at the University of Maryland (<http://glcf.umiacs.umd.edu>). We downloaded a MODIS Tree canopy cover data set for year 2001 (V003) from the latter site (last accessed 20 February 2008) with a geographic coordinate system and reprojected it to LAEA (Fig. 5.1).

The distribution of VCF tree cover across the region (Fig. 5.1) provides additional corroboration for the presence of trees in the areas where GLC-2000 and MODIS.PFT both identify tree-dominated cover: these are the areas with high values of VCF tree cover. The areas of disagreement between the two compared categorical maps tend to be those with low tree cover on the MODIS.VCF map (Fig. 5.1). Overall, the open-canopy forests dominate the region with 42% of the total land area having tree canopy cover between 10 and 40% while only 7% of the land area has tree-canopy cover of 65% and higher (Fig. 5.2). The total area of tree-canopy cover derived from MODIS.VCF product for lands north of 60° is 1977 thousand km² (Fig. 5.3).

Another VCF-type product relies on the probability method which was originally developed for mapping forest extent in the pan-European region (i.e., all Europe up to the Ural Mountains) using the AVHRR instrument data of the NOAA series satellites (Häme et al. 2000, 2001; Paivinen et al. 2001; Schuck et al. 2002). The target variables, including proportions of coniferous, broadleaved and mixed forest were estimated within 1-km² units. Forty eight (48) AVHRR images were collected from summer 1996 and one image from 1997. The images were calibrated into

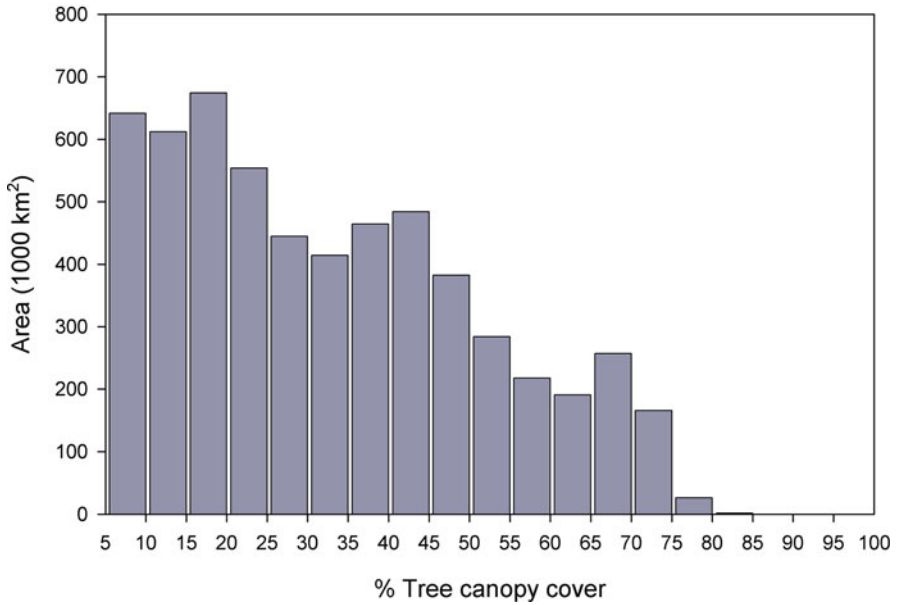
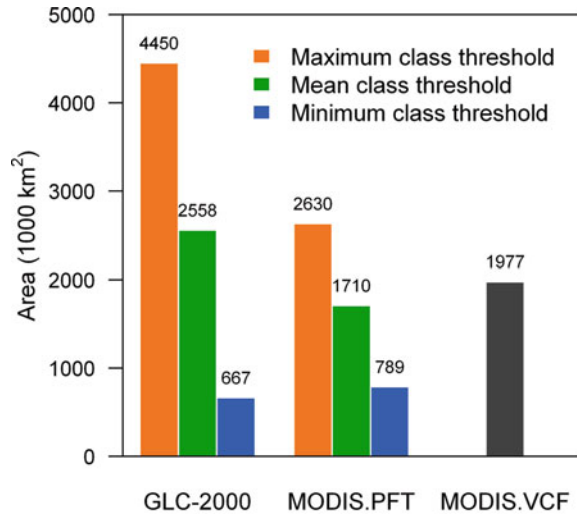


Fig. 5.2 Histogram of tree-canopy cover in the Eurasian Arctic from MODIS.VCF for canopy cover greater than 5%

Fig. 5.3 Representation of the total tree-covered area on GLC-2000, MODIS.PFT, and MODIS.VCF



spectral reflectance values by applying the SMAC atmospheric correction (Rahman and Dedieu 1994) and a BRDF correction using Roujean model (Wu et al. 1995). A mosaic was compiled using the radiometrically and geometrically corrected images. The average reflectance of overlapping pixels was computed after applying an automatic cloud screening algorithm.

The probability method includes an unsupervised image classification as a preliminary step. For the classes of unsupervised clustering a reference data sample was selected from the European CORINE land cover data base that was available from the central and southern European region (CORINE 1993). The sample comprised squares of 500 m by 500 m within which the tree species proportions were computed. The sampling was done using three strata: Mediterranean region, Atlantic region, and continental temperate region. No CORINE reference data was available from the boreal or arctic region.

The multi-normal density functions of the spectral classes from unsupervised clustering and the reference data values for the same classes were combined using the probability algorithm (Häme et al. 2000, 2001). The estimated values of the forest area were compared with the official EUROSTAT (1998) forestry statistics and with the national-level forest inventory statistics in selected countries. They also were calibrated to match district-wise with those statistics (Päivinen et al. 2001). Based on calibrated map, the total area of conifer-dominated forest north of 60° in Europe is 995,013 km² and broadleaf-dominated forest is 190,191 km². At country level in the boreal zone (most of Sweden belongs to the boreal vegetation zone) the AVHRR-based forest area estimation matched with the statistical data well (Fig. 5.4). Also at sub-national level within Finland agreement was relatively good (Fig. 5.5). At a sub-district level, the AVHRR map underestimated the coniferous and broadleaved forest areas in Finland (Fig. 5.6). The likely reason for this was the different nomenclatures in the Finnish national forest inventory and CORINE.

The comparison of MODIS.VCF and AVHRR.VCF map indicates reasonably good agreement in the southern part of northeastern Europe and increasing disagreement further north (Fig. 5.7a). The abrupt northern boundary on AVHRR.VCF

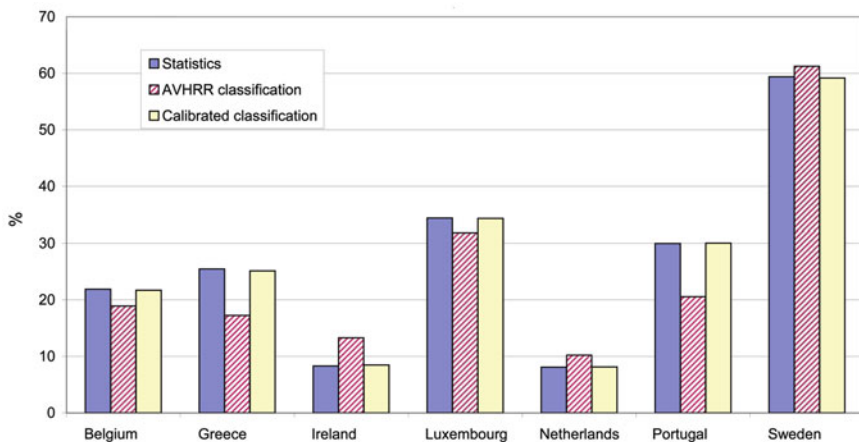


Fig. 5.4 Comparison of EUROSTAT forest statistics and calibrated and uncalibrated AVHRR.VCF forest cover estimates in some European countries (from Paivinen et al. 2001). Reproduced by permission of European Forest Institute

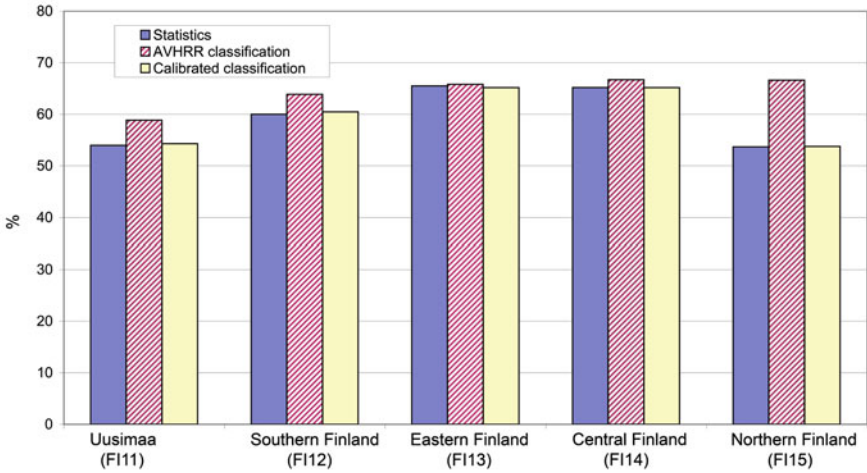


Fig. 5.5 Comparison of EUROSTAT forest statistics and calibrated and uncalibrated AVHRR.VCF forest cover estimates within districts in Finland (virtually the entire territory of Finland is above 60°N; from Paivinen et al. 2001). Reproduced by permission of European Forest Institute

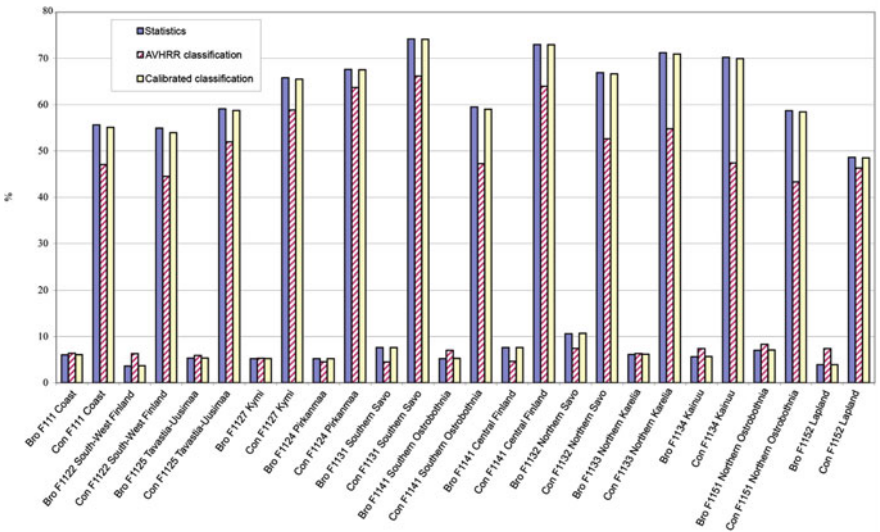


Fig. 5.6 Comparison of Finnish National Forest Inventory statistics within sub-districts and calibrated and uncalibrated AVHRR.VCF estimates of the proportion of conifer and broadleaf tree-cover (mixed forest class excluded from AVHRR classification values; split between broadleaved and conifer types in calibrated classification values to match inventory statistics; from Paivinen et al. 2001). Reproduced by permission of European Forest Institute

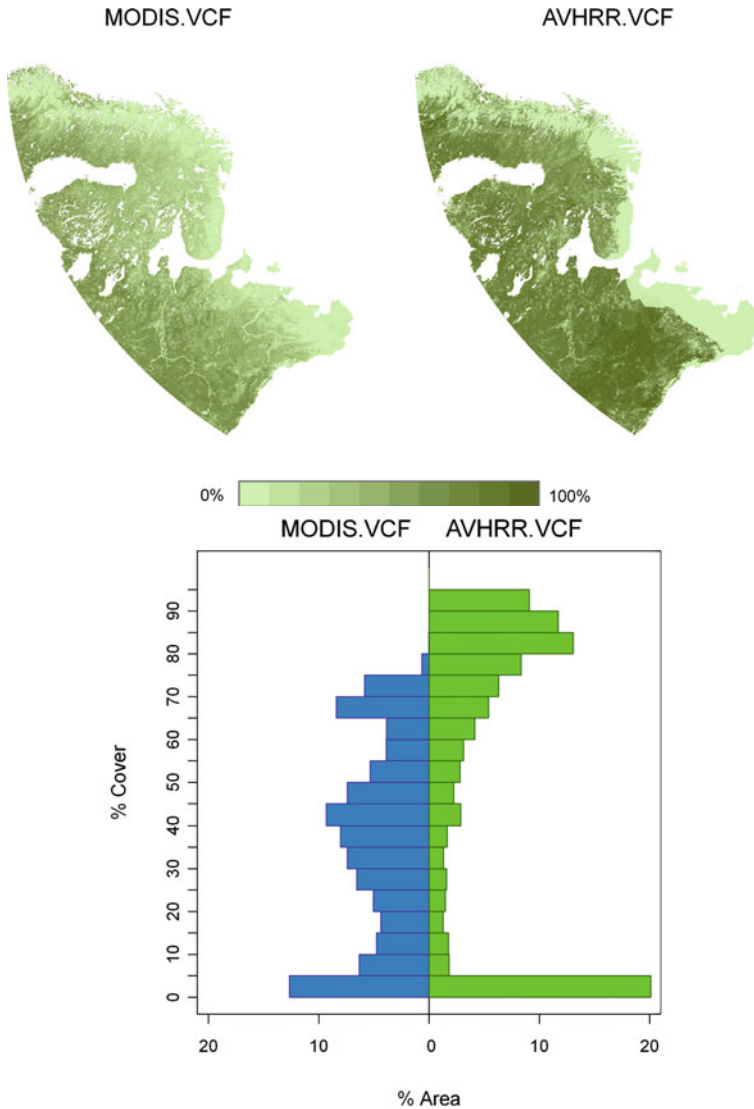


Fig. 5.7 Continuous field products for North-Eastern Europe: (*top*) Distribution of percent tree-canopy cover on MODIS.VCF map and percent forest cover on AVHRR.VCF map; (*bottom*) histogram for MODIS.VCF and AVHRR.VCF

map reflects the northern tree line that was extracted from the literature and applied before calibrating the continuous estimates using the Eurostat statistics. The total area of tree crown cover is projected to occupy 36% by MODIS.VCF whereas percent forest cover based on AVHRR.VCF is 55%. Differences in definitions of the mapped variable appear to account for most of the difference in the results. The percent tree crown cover approximately corresponds to 0.8 of percent canopy cover

(Hansen et al. 2003a); taking this adjustment into account the MODIS.VCF estimate of crown cover is approximately 45%, which is still lower than AVHRR.VCF estimate. Furthermore, CORINE definition of “forest” includes lands with >15% tree-canopy cover (Heiskanen 2008); thus pixels with as low as 15% tree cover would be classified as “100% forest” if this tree cover is distributed evenly across the pixel. The more open tree canopies tend to be, the greater the disagreement between the two products can be expected due to differences in definition of the continuously mapped variable. This explains the increasing disagreement as one moves further north, the overall higher area estimate, and the greater proportion of pixels with high percent tree cover on AVHRR.VCF (Fig. 5.7b). The comparison of MODIS.VCF maps with a detailed biotype map in northern Finland indicated that the MODIS.VCF map underestimated in areas with high forest cover and overestimated in areas with low tree cover, particularly on mires (Heiskanen 2008).

5.2.3 Comparison of Tree Cover Representation on Coarse Resolution Maps

Certain characteristics of tree cover in Arctic Eurasia make the categorical mapping challenging, including large areas occupied by open low-stature trees with heights close to the lower boundary of the “tree” definition (3–5 m) and the significant presence of other (non-tree dominated) land-cover types within 1-km pixels. However, the estimates of the total tree-canopy cover for the Arctic region of Eurasia agree better among the examined land-cover products than the results of per-pixel spatial disagreement may suggest (Table 5.2). The MODIS.VCF estimate of regional total tree-canopy cover (22% of the total land area) is lower than the tree-dominated area estimate from GLC-2000 (50%) or MODIS.PFT (30%), although it is closer to the MODIS.PFT estimate. However, the three estimates are not directly comparable. While the total VCF tree cover is an estimate of the area of tree-canopy cover, the tree-dominated area estimates from the categorical maps include land surface not covered by tree canopies. This is especially significant in regions with open forests because land with canopy cover as low as 15% is still defined as tree-dominated by legends of categorical maps. The tree-cover estimate derived from MODIS.VCF is consistent with this difference in definitions and suggests that categorical maps may over-represent tree cover for the region primarily as a result of their inability to capture the sub-pixel scale variations in tree cover. In the GLC-2000 data set, tree-dominated pixels are defined to have tree-canopy cover between 15 and 100% (57.5% mid-range). In the MODIS.PFT classification, forests are defined as pixels where tree cover dominates over shrub, herbaceous or non vegetated land cover, which could be as low as 30% or as high as 100% (65% mid-range). Therefore, estimates of tree canopy cover derived from the categorical maps could theoretically range anywhere between the minimum and maximum thresholds of the class definitions (Fig. 5.3). Canopy cover estimates using the mid-range value of tree class from the categorical data sets compare well with the MODIS.VCF tree cover estimate. Note however, that the actual distribution of tree cover within the classes is

unknown, so the actual mean tree cover might be lower or higher than the class mid-range. Considering the known prevalence of open-canopy tree stands in the region (Fig. 5.2), the actual mean value of tree cover in tree-dominated pixels is likely to be lower than the mid-range values. If we translated MODIS.VCF dataset to discrete classes and estimated the total tree-dominated area following GLC-2000 definition (i.e., counted all pixels with VCF tree cover >15% as tree-dominated) it would be 5,174 thousand km² compared to 4,550 thousand km² actually mapped by GLC-2000; for MODIS.PFT the relevant values are 3,334 and 2,630 thousand km², respectively. Thus when class definitions are aligned, the MODIS.VCF product suggests greater area with tree cover than either of the two examined categorical maps; the difference is 13% for GLC-2000 and 27% for MODIS.PFT and indicates either an omission of low-canopy cover forests from GLC-2000 and MODIS.PFT or commission (overestimation) in the VCF map.

Open-canopy tree cover is very common not only in Northern Eurasia but in the entire Arctic. Interestingly, the global and regional GLC-2000 legends separate closed and open broadleaf deciduous trees, thus allowing representation of tropical savannas but not the open-canopy needle-leaf tree cover in the Arctic region. This may indicate the lack of attention from map developers to the Arctic region and to a vegetation type that has an important control over feedback mechanisms to climate change, including albedo and carbon cycling (McGuire et al. 2007). In selecting the suitable map for the region the availability of open-canopy needle-leaf tree class can be an important feature which is available on some maps (e.g., MODIS.IGBP). The open-canopy needle-leaf tree cover class would be important to include in future mapping programs aimed at improving the utility of land-cover maps for global change research in the Arctic.

5.3 Comparison of Coarse Resolution Maps with Landsat-Based Land Cover

The cross-comparison of the GLC-2000 and MODIS.PFT map revealed areas of uncertainty, geographically and thematically. However, analyses of agreement and disagreement between coarse resolution maps provide only an indirect measure of class confidence. Independent validation and accuracy assessment has long been recognized as an important challenge for all land-cover products (Morissette et al. 2002; Stahler et al. 2006). Since there is a paucity of validation data in the Arctic, this challenge will likely persist. To obtain some indication of the products' performance in Northern Eurasia we compared the coarse resolution maps with Landsat-based land-cover maps at two validation sites. The two site maps were developed as part of an ongoing, broader effort to validate land-cover maps within the region (Northern Eurasia Land Cover Dynamics Analysis (NELDA) project <http://www.fsl.orst.edu/nelda/index.html>). Dominant vegetation cover data from GLC-2000 and MODIS.PFT were compared with medium resolution (28.5 m) land-cover maps developed for two sites: Komi (66°55' N, 55°35' E) and St. Petersburg (59°45' N, 31° 11' E). Land-cover maps for the two sites were produced from ground inventory

data and Landsat Enhanced Thematic Mapper Plus (ETM+) data. The imagery was first orthorectified using an automated procedure (Kennedy and Cohen 2003) and then radiometrically corrected to remove atmospheric scattering effects (Chavez Jr 1996; Canty et al. 2004). The legends for the two maps followed the LCCS classification scheme (Di Gregorio 2005) and were recoded into the DVT classes: tree, shrub, herbaceous vegetation, and barren or sparse vegetation (Fig. 5.8). The LCCS classification defines “tree dominated” cover as land with greater than 15% tree cover, where trees are woody vegetation taller than 5 m or trees taller than 3 m. Similarly, shrub and herbaceous dominated vegetation types have a minimum of 15% plant cover, respectively. However, the dominance of a life form is defined hierarchically by the height of the canopy layer, which ranges from trees to shrubs to herbaceous plants. Thus, a landscape with a top canopy layer represented by trees with canopy cover >15% (for example 20%) and a sub layer represented by shrubs with a canopy cover of 40% will be classified as “tree dominated”. Lands with less than 15% vegetation cover are labeled as “bare land and sparse vegetation”.

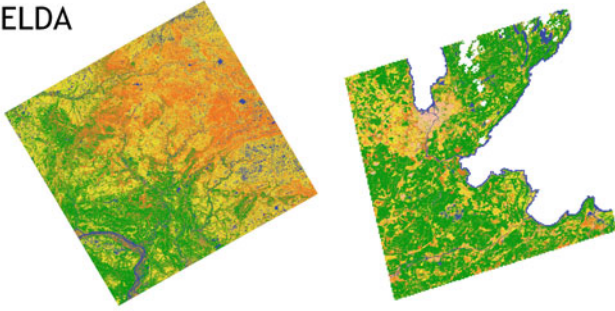
5.3.1 Komi Site

The Komi test site is located in the subarctic climate zone in the northeast of European Russia. The climate is continental with brief summers, long winters and a daily average temperature below 0°C during 227 days a year. Mean annual temperature varies between −3 and −5°C. The mean temperature in July is 12.3°C, in January it is −18.9°C. The snow cover lasts on average for 225 days (3 Oct–1 Jun); the annual precipitation is 430–436 mm year^{−1}; 30% is snow. Severe climate, excessive moisture, relatively flat terrain and seasonally-frozen ground (and permafrost) determine the high degree of soil water saturation and presence of many wetlands. The site is located in the forest-tundra zone. Tundra communities are dominated by dwarf-birch (*Betula nana* L.) and willow species (*Salix glauca*, *S. lanata* and *S. phylicifolia*). Further south, forest-tundra and northern taiga communities mainly consist of Siberian spruce (*Picea obovata* Ledeb.) and birch species (*B. tortuosa* or *B. pubescens*). The density of human population is low. The traditional land use is reindeer herding and in recent years the extraction of vast resources of carbohydrates from terrestrial and shelf deposits of the Timano-Pechorsk oil-gas province became the second major human impact. Wild fire is also a significant factor in vegetation dynamics.

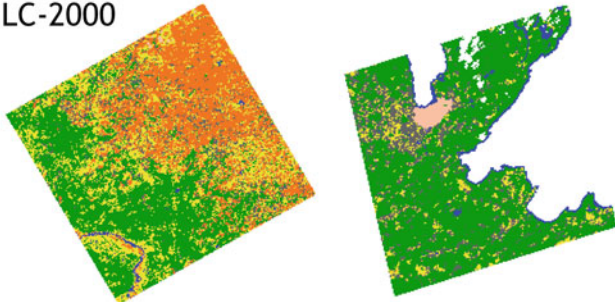
The analysis of vegetation distribution was based on a Landsat ETM+ image from June 8, 2000 (WRS-2 path 172, row 13, UTM projection, zone 40). Twelve vegetation cover classes (plus water) were identified using supervised classification and these were aggregated to the dominant vegetation types used in this study (Fig. 5.8). Map accuracy was assessed using forest inventory and other ground truth data. The overall agreement with of DVT map with the ground data is 84.3% (kappa = 68.6%).

At the Komi site, the overall agreement between GLC-2000 and MODIS.PFT is 65%. The spatial distribution of tree-dominated vegetation mapped on all

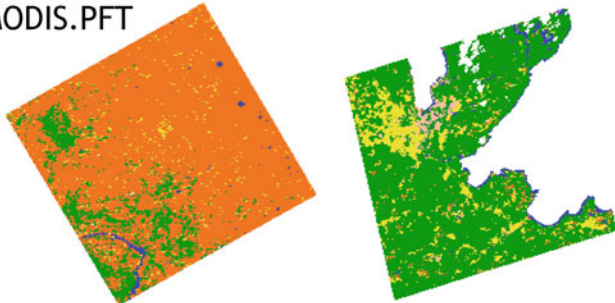
NELDA



GLC-2000



MODIS.PFT



MODIS.VCF

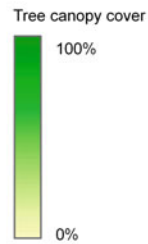
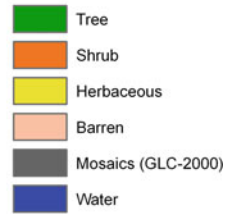
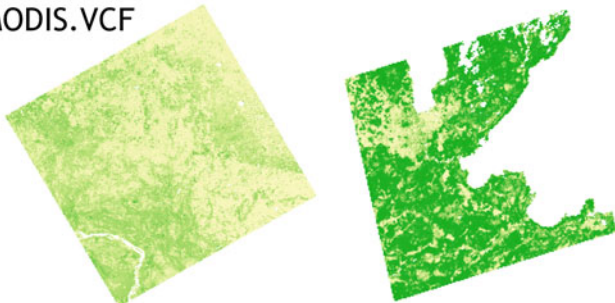


Fig. 5.8 (*Left column*) Dominant vegetation types at Komi site and (*right column*) St. Petersburg site mapped by NELDA, GLC-2000, MODIS.PFT, and MODIS.VCF

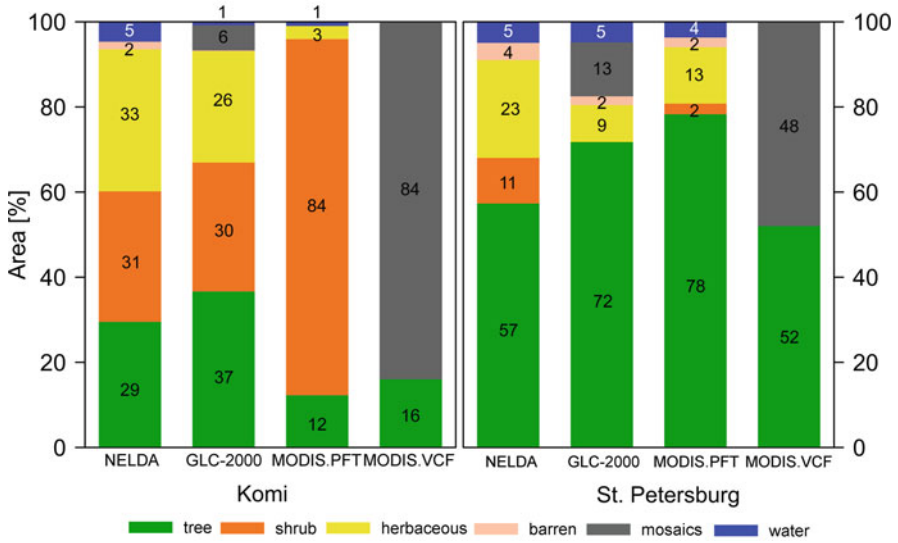


Fig. 5.9 (Left) Composition of dominant vegetation types at Komi site and (right) St. Petersburg site as mapped by NELDA, GLC-2000, MODIS.PFT, and MODIS.VCF

coarse-resolution products is in general agreement (Fig. 5.8) but the area proportion of tree-dominated vegetation mapped by MODIS.PFT (12%) and MODIS.VCF (16%) is lower than the NELDA reference map (29%, Fig. 5.9). In comparison, the area occupied by tree vegetation on GLC-2000 map is higher (37%). Furthermore, with 84% of the area mapped as shrubs, MODIS.PFT fails to distinguish between shrub and herbaceous vegetation. The confusion between tree and shrub is the most common disagreement at the Komi site, and it occupies 27% of the total mapped area. The second most common type of confusion is between shrub and herbaceous vegetation (6% of total area). Both MODIS.PFT and GLC-2000 underestimate the area occupied by water bodies (1% compared to 5% mapped by NELDA). While water covers only a small fraction of the land surface, it is very important ecologically as changes in arctic lakes are an important indicator of permafrost dynamics (e.g., Frohn et al. 2005). Improved region-wide mapping of terrestrial water bodies is clearly important.

5.3.2 St. Petersburg Site

The St. Petersburg test site is located in northwestern Russia at the southern boundary of the study region. The site has a maritime climate, with cool wet summers and long cold winters. Mean temperature ranges from 16 to 18°C in July and -7 to -11°C in January. The mean daily temperatures are below zero from

November until March. Annual precipitation is 600–800 mm. The natural vegetation of the area is southern taiga: major dominant conifer species include Scots pine (*Pinus sylvestris* L.) and Norway spruce (*Picea abies* (L.) Karst.), growing in both pure and mixed stands. After disturbance, these species are often replaced by northern hardwoods, including birch (*Betula pendula* Roth.) and aspen (*Populus tremula* L.). The site is part of the East-European Plain; the terrain is flat and consists of ancient sea sediments covered by a layer of moraine deposits. Toward the northwest, glacial features dominate the landscape and bedrock topology is more prominent. Soils are mostly podzols on deep loamy to sandy sediments. The site has a long history of agricultural and forest management dating from the eighteenth century. The human population of the region is close to 7 million, with over 5 million people living in the city of St. Petersburg (Krankina et al. 1998).

Land cover was mapped using a nearly cloud-free Landsat ETM+ image from June 2, 2002 (WRS-2 path 184, row 18, UTM Zone 36 N, WGS84). After geometric and radiometric correction, the image was transformed into Tasseled Cap indices of brightness, greenness, and wetness (Crist 1985). Using an iterative unsupervised classification of the Tasseled Cap image, maps of land cover were created at different hierarchical classification levels starting with the 5 DVT classes that were then broken up into 17 more detailed classes. Forest inventory data (Kukuev et al. 1997) and expert-classified reference polygons were used for accuracy assessment. For 17 classes the agreement with reference data was 66.6% ($\kappa = 61.4\%$). At the level of dominant vegetation type the agreement with reference data is near-perfect 98.5% ($\kappa = 95.6\%$).

At the St. Petersburg site, the overall agreement between GLC-2000 and MODIS.PFT is high at 83%. The landscape is very fragmented and GLC-2000 mapped 13% of the site as mosaics of tree, shrub and herbaceous (including croplands) vegetation possibly inflating the calculated percent agreement with MODIS.PFT (Table 5.1, Fig. 5.8). The tree cover is overestimated by the GLC-2000 map (72%) and MODIS.PFT map (78%) when compared to NELDA (57%; Fig. 5.9). In comparison, the MODIS-VCF estimate of 52% tree cover is in good agreement with NELDA, but as explained in the regional analysis (see 5.2.3), the results for categorical maps and VCF are not directly comparable. By far the most common confusion type at the St. Petersburg site is between trees and herbaceous vegetation (8% of total area). One likely cause for this confusion is the significant presence of peatlands and other wetlands at the St. Petersburg site, with their characteristic mix of open canopy trees, low shrubs, and a moss-dominated herbaceous layer (Krankina et al. 2008). These complex plant assemblages fit poorly in class definitions of land-cover maps (Frey and Smith 2007). Both GLC-2000 and MODIS.PFT underestimate the extent of shrubs and herbaceous vegetation in the overall land cover of the St. Petersburg site (Fig. 5.9).

5.4 Effects of Vegetation on Carbon Stores in Terrestrial Ecosystems of Arctic Eurasia: Major Controlling Factors and Sources of Uncertainty

Information on land cover is among the principal inputs for simulation modeling, which is a fundamental tool for understanding ecosystem responses to climate and disturbance and extrapolating these processes over time and space. Here, we discuss the results of a re-analysis of the terrestrial C budget for Arctic Eurasia over the last decade (1997–2006) for different vegetation types of the region. The Terrestrial Ecosystem Model (TEM; Raich et al. 1991) was driven by spatially- and temporally-explicit climatology, disturbance, and land-cover/land-use data sets with the objective of determining the role that different vegetation and ecosystem types play in the regional terrestrial C balance in response to changing atmospheric CO₂ concentration, climate variability, ecosystem type, fire, forest management and agricultural land use.

We simulated 1,000+ years of C dynamics for potential vegetation over Arctic Eurasia with CO₂ fertilization effects, variable climate and transient disturbance and land use. The TEM is calibrated to site-specific vegetation parameters and extrapolated across the study area based on a 0.5° latitude x 0.5° longitude grid matching the input climate data sets (Climate Research Unit, University of East Anglia, UK; Mitchell and Jones 2005). The model was run on a monthly time-step at sub-grid resolution based on a non-spatial mosaic of “cohorts” representing unique vegetation types and disturbance histories within each grid cell. Additional methodological details on TEM, the input data sets, and the simulation framework are given in Chapter 6 (this volume).

The input potential vegetation data set was derived from the Global Land Cover Characterization (GLCC; Loveland et al. 2000) version 2 Seasonal Land Cover Regions (SLCR) Eurasia data set at 1-km (equal-area) resolution. Among the various vegetation data sets available for this region (see Section 5.2, above), the GLCC.SLCR map was chosen for its detail in classification (200+ categories) and its description of vegetation mosaics, thereby allowing flexibility in translating for the arctic conditions, boreal and temperate ecosystem types for which the TEM is calibrated. The translated vegetation map, which included 10 upland categories, was aggregated to the 0.5° grid, but retaining the area represented by each unique vegetation type within a grid cell as an individual, non-spatial cohort. Wetland cohort areas were assigned to each grid cell based on a 1° × 1° grid cell fraction inundated database (Matthews and Fung 1987), where wetland area equals the product of fraction inundated and total cell area. The final classification, then, contained 17 categories (in addition to water, ice, and barren; Table 5.3) of upland and associated wetland vegetation types (some ecosystem types, such as polar desert and xeric shrublands, were not allowed to have wetland associates). Although at a relatively coarse resolution (0.5°), the cohortized potential vegetation map was designed to capture upland vegetation community type mosaics and their transitions across spatial gradients, along with spatially-explicit data on wetland extent and type.

Table 5.3 Classification scheme and areas represented by the ecological zones for Eurasian Arctic (north of 60°N) as input data for the TEM simulations. In parenthesis is the four-letter code for each ecozone; it is followed, in quotations, by its assigned dominant vegetation type (DVT) for comparison with the other vegetation maps considered in [Chapter 5](#)

Ecological zone	Area (km ²)
Inland water	372,877
Ice, rock, “Barren”	2,337,878
1 Prostrate Tundra / Polar Desert (PTPD), “Herbaceous”	1,782,272
2 Arctic Shrub Tundra (ASHT), “Shrub”	1,638,383
3 Arctic Shrub Tundra Wetlands (ASHTw), “Shrub”	678,759
4 Boreal Needleleaf Evergreen Forest (BNEF), “Tree”	1,128,228
5 Boreal Needleleaf Evergreen For. Wetlands (BNEFw), “Tree”	530,967
6 Boreal Needleleaf Deciduous Forest (BNDF), “Tree”	1,229,673
7 Boreal Needleleaf Deciduous For. Wetlands (BNDFw), “Tree”	489,069
8 Boreal Broadleaf Deciduous Forest (BBDF), “Tree”	740,583
9 Boreal Broadleaf Deciduous Forest Wetlands (BBDFw), “Tree”	67,061
10 Temperate Needleleaf Evergreen Forest (TNEF), “Tree”	469,347
11 Temperate Needleleaf Evergr. Forest Wetlands (TNEFw), “Tree”	65,643
12 Temperate Broadleaf Deciduous Forest (TBDF), “Tree”	60,732
13 Temperate Broadleaf Decid. For. Wetlands (TBDFw), “Tree”	2,724
14 Xeric Woodlands (WOOD), “Tree”	4,291
15 Xeric Shrublands (XESH), “Shrub”	155,577
16 Grasslands (GRAS), “Herbaceous”	163,691
17 Grasslands / Herbaceous Wetlands (GRASw), “Herbaceous”	11,310
Total inland area	11,929,065

The location and timing of disturbances are determined from data sets on fire occurrence, area burned, fire severity, and fire return interval, as well as modeled data for rates of forest harvest and crop and pasture establishment and abandonment. The annual area burned data set for Eurasia was based on AVHRR satellite-derived fire scars data from 1996–2002 (Sukhinin et al. 2004) and backcasted to the year 1000 based on 0.5° resolution fire return intervals. For a complete description of the historical fire data set, fire return interval calculation, and backcasting approach, see Balshi et al. (2007). That study’s fire database was extended from 2002 to 2006 for Northern Eurasia using the Global Fire Emission Database version 2 (van der Werf et al. 2006). The data set provides monthly burn fraction by 1° × 1° grid cell, which was converted to annual burn area and extracted from cohorts based on a priority list of burnable ecosystem types, thereby creating a new, secondary cohort of age zero for that year. In the same way, forest harvest and land use (crops or pasture) cohorts were created in the input data set, derived from 1° × 1° gridded, annual land use transitions data for years 1700 through 2000, modeled by Hurtt et al. (2006).

The model produced monthly estimates of C stocks in vegetation, soil and product pools for each cohort over the length of the simulation, which we report as average annual total ecosystem C stocks across all cohorts within each ecozone, and average these values over the 10-year analysis period (1997–2006). The average annual change in C stocks reported here represents the Net Ecosystem C Balance

(NECB) of the system (see Chapin et al. 2006). NECB includes both the C flux from the terrestrial system to the atmosphere through the initial conversion flux (e.g. from fire) and subsequent decomposition of reactive soil organic matter and decay of post-harvest product pools as well as the lateral leaching flux of dissolved organic C via stream export.

We summarized the disturbance data and their effects (along with CO₂ and climate) on total ecosystem C stores and average annual balance by ecozone across the study area for the 1997–2006 time period (Table 5.4). The simulation shows that the study area as a whole is losing C from terrestrial ecosystems on an average rate of 44 Tg C year⁻¹ from 1997–2006. The system is estimated to contain total ecosystem C stocks (in vegetation, soils, and product pools) on the order of 266 Pg C. More than 167,000 km² were burned over this decade (about 2% of the total study area), with another 119,000 km² of forest harvested (~2.5% of forest area) and 72,000 km² (less than 1% of the total study area) in agricultural land use (crops and pastures). The majority of area burned occurred in larch-dominated forests of eastern Siberia (Boreal Needleleaf Deciduous Forest, BNDF, ecozone), with an average 0.6% of its area burned annually during this time period. The results show this ecozone as having the majority contribution toward the overall C loss in the study area. The BNDF ecozone alone is losing more C than the study area as a whole, suggesting that the rest of the ecozones combined acted as a net C sink (of about 21 Tg C year⁻¹) over this decade. Most of the strength of that sink is found in the tundra types (Prostrate Tundra/Polar Desert, PTPD, and Arctic Shrub

Table 5.4 Disturbance area and C stocks for each ecozone and land use type in the Eurasian Arctic for the period 1996–2006. Wetland types were merged with their upland counterparts to present these data by ecozones

Ecozones	Area ^a (km ²)	Area harvested ^b (km ²)	Area burned ^b (km ²)	Total (Tg C)	Density (kg C m ⁻²)	Change in stocks ^c (Tg C year ⁻¹)
PTPD	1,774,437	0	1,788	30,255	17.05	8.75
ASHT	2,312,690	0	5,338	63,991	27.67	17.93
BNEF	1,654,928	41,778	25,379	26,556	16.05	-16.81
BNDF	1,717,593	12,726	104,436	123,271	71.77	-65.03
BBDF	797,853	7,918	14,336	11,275	14.13	3.57
TNEF	517,291	47,148	1,478	3,755	7.26	7.55
TBDF	49,802	9,551	18	972	19.51	-0.06
WOOD	3,369	0	77	66	19.73	0.01
XESH	153,642	0	7,628	3,581	23.31	-0.33
GRAS	164,299	0	7,167	1,439	8.76	-1.25
CROP	41,489	0	0	522	12.54	1.09
PAST	30,917	0	0	146	4.73	0.09
Total	9,218,310	119,121	167,645	265,828	28.84	-44.49

^aArea represented by each ecozone or land use in year 2006.

^bArea harvested or burned for each ecozone during the period 1996–2006.

^cAll C values are given as the 10-year average between 1996 and 2006.

Tundra, ASHT). The majority of the forest harvest area occurred in temperate and boreal pine and spruce forests (Temperate Needleleaf Evergreen Forest, TNEF, and Boreal Needleleaf Evergreen Forest, BNEF, ecozones). With relatively small area burned, the temperate part (TNEF) located primarily in the western portion of the study region is estimated to be sequestering C at a rate of $7.6 \text{ Tg C year}^{-1}$, while the boreal part (BNEF), with higher rates of fire, is losing C at nearly $17 \text{ Tg C year}^{-1}$.

The C budget for the ecozones of Northern Eurasia over the past decade assembled here, when compared with the disturbance data, suggests some of the potential controlling factors on the sources and sinks of C in this region. The ecozones losing the most C over the time period also had the largest burned area, thus fire appears to have a substantial effect on C loss from the system. The very large area burned in the larch-dominated forests (BNDF ecozone) combined with its high C density (more C available to be released during and after fire) to produce the vast majority of the C source for the study area. The tundra ecozones (PTPD and ASHT) represent a large and mostly undisturbed area that may be responding to changes in climate in producing a net C sink.

5.5 Significance of the Current Uncertainty in Vegetation Cover for Estimating Carbon Stores, Sources, and Sinks in Terrestrial Ecosystems

The analysis in Section 5.4 shows that the different ecozones have large variation in their C stocks and fluxes, indicating that the underlying vegetation map used to drive model simulations can have important consequences for regional C budget estimates. To assess the effect of different input vegetation data sets on the modeled estimates of regional C balance, we performed a simple analysis in which we produced estimates of live vegetation and total ecosystem C density and mean estimates of per-area change in C stores for each ecozone from our simulations (Table 5.4). The density and change estimates incorporate the “average” effects of CO₂, climate, and disturbance at the ecozone level. We then aggregated the ecozones to the broader DVT categories (see Table 5.3) and used the per-area stock and flux estimates to extrapolate across each DVT category according to the area represented by these categories in the ecozone classification used in this study (Table 5.3) as well as in the GLC-2000 and MODIS.PFT maps (Table 5.2). This “bookkeeping” type approach to regional C budget analysis assumes average, constant effects of climate and disturbance within each DVT. While this is admittedly a very simplistic approach, it does provide the first approximation of the effect of input vegetation data sets on the modeled estimates of regional C balance.

The GLCC-based vegetation classification (Loveland et al. 2000) used in C modeling for this study agrees more closely with the GLC-2000 than the MODIS.PFT in terms of the total areas represented by the DVT categories, particularly with the tree and shrub estimates (Table 5.5). Note also that C simulation considered a larger

Table 5.5 Comparison of the effect on regional C balance estimates of extrapolating simulated C stock and flux density across the different area estimates of the dominant vegetation type categories (DVT) from the classifications discussed in this chapter (A – live vegetation C, B – total ecosystem C)

A	Simulated averages				GLCC				GLC-2000				MODIS.PFT				
	Density	Density Δ	Area	Total	Density Δ	Area	Total	Δ in Stocks	Area	Total	Δ in Stocks	Area	Total	Δ in Stocks	Area	Total	Δ in Stocks
Tree	5.043	0.032	4,741	24	0.15	4,450	22	0.14	2,630	13	0.08	2,630	13	0.08	2,630	13	0.08
Shrub	0.651	0.022	2,466	2	0.05	2,258	1	0.05	5,290	3	0.12	5,290	3	0.12	5,290	3	0.12
Herb.	0.387	0.003	2,011	1	0.01	916	0	0	680	0	0	680	0	0	680	0	0
Barren	0	0	2,338	0	0	1,232	0	0	255	0	0	255	0	0	255	0	0
Total	2.832	0.023	11,556	26	0.21	8,856	24	0.2	8,855	17	0.2	8,855	17	0.2	8,855	17	0.2
B	34.992	-0.149	4,741	166	-0.7	4,450	156	-0.66	2,630	92	-0.39	2,630	92	-0.39	2,630	92	-0.39
Shrub	27.398	0.071	2,466	68	0.18	2,258	62	0.16	5,290	145	0.38	5,290	145	0.38	5,290	145	0.38
Herb.	16.091	0.042	2,011	32	0.09	916	15	0.04	680	11	0.03	680	11	0.03	680	11	0.03
Barren	0	0	2,338	0	0	1,232	0	0	255	0	0	255	0	0	255	0	0
Total	28.783	-0.05	11,556	266	-0.44	8,856	232	-0.46	8,855	248	0.02	8,855	248	0.02	8,855	248	0.02

Units: Density (kg C m^{-2}); density Δ ($\text{kg C m}^{-2} \text{ year}^{-1}$); Area (103 m^{-2}); Total C stocks (Pg C); Δ in stocks (Pg C year $^{-1}$).

overall study area than the map analysis from Section 5.2 (11.8 million km² in C simulation compared to 8.9 million m² in the two maps). However, the difference is primarily in areas of the Herbaceous and Barren DVT types because GLCC-based map included all areas above 60°N latitude whereas the GLC-2000 and MODIS.PFT maps did not include areas above 74°N – most of which is dominated by herbaceous vegetation (PTPD) and Ice, Rock (Barren) types.

While all three C budgets produce similar estimates of total ecosystem C stocks for the region, the estimated average annual change in C stocks (i.e. terrestrial C balance) over the last decade differs substantially for the MODIS.PFT classification as compared with the other two (Table 5.5). Extrapolations based on the vegetation data used in C simulation and the GLC-2000 actually produced very similar estimates of regional C balance (−0.44 and −0.46 Pg C year^{−1}, respectively), primarily because of the similarity in areas of the tree and shrub categories. While these two estimates suggest a substantial loss of C from this region during the 1997–2006 time period, the extrapolation based on the MODIS.PFT classification resulted in a more neutral C balance estimate (a small net sink of 20 Tg C year^{−1}). This result is due to the higher estimate of shrub area, which acts as a C sink in our simulations and offsets the lesser area of C loss from the tree cover category.

The impact of the input vegetation data appears even more significant when live vegetation C is examined separately (Table 5.5b). The estimate of C stock in live vegetation based on the GLC-2000 map (24 Pg C) is 40% higher than the estimate based on the MODIS.PFT map (17 Pg C). While the estimates of the overall change in live vegetation C stocks are very similar for both maps (0.2 Pg C sink), the attribution of the projected C sink is quite different depending on the map used: based on GLC-2000 map most of the C accumulation occurs in tree-dominated ecosystems while MODIS.PFT map would attribute most of the C sink to shrub vegetation.

This extrapolation provides only a general sense of the effect that different input vegetation data sets will have on estimates of C stocks and flux. A more comprehensive, quantifiable estimation of these effects would require new simulations in which the different vegetation maps were incorporated into the spatially-explicit data sets used to drive the model. In this analysis, for example, the near-neutral C balance estimate based on the MODIS.PFT classification does not fully capture the effects of fire because of the lower estimate of tree-cover area in this map. More explicitly connecting this data set with the fire data would more realistically distribute area burned across the study region, including fires in shrub-dominated area. This may alter the overall MODIS.PFT-based estimate of NECB for the region.

5.6 Summary and Conclusions

Significant differences exist between land-cover maps of Arctic Eurasia even at relatively coarse resolution and at the level of broad plant functional and dominant vegetation types. Thus, the choice of a specific land-cover product can have a major impact on the results of many research projects in the region and this source of uncertainty is often overlooked. The distinct geographic patterns of differences

indicate the areas where the effects of map selection can be the greatest and where further improvements in mapping are needed. The discrepancies in categorical maps are concentrated at borders between biomes and in parts of the region where significant presence of open canopies of woody plants (trees and shrubs) or herbaceous vegetation is expected.

Overall, the extent of disagreement between the compared categorical maps is greater in Siberia and Far East than in the western part of Arctic Eurasia. The paucity of ground data and the presence of larch (deciduous conifer) in the eastern part of the study region may be responsible. However, the high level of confusion between the two compared land-cover maps at the treeline and further north is prevalent throughout the region. This geographic distribution of disagreement may reflect the limitation of coarse resolution categorical maps in representing open vegetation covers and mixed or fragmented landscapes. Vegetation continuous field maps of dominant vegetation types are a promising alternative to categorical maps.

The agreement among the compared maps is highest for tree-dominated vegetation, which is represented more consistently than other vegetation-cover types in the categorical maps. Tree-cover representation in the MODIS.VCF product corroborates the general pattern of agreement in tree-cover distribution between the two categorical maps. Furthermore, the estimates of the total area of tree-dominated vegetation cover in the study region agree reasonably well among the three maps (GLC-2000, MODIS.PFT, and MODIS.VCF). The degree of spatial agreement is the lowest for herbaceous vegetation. One of the reasons for that may be the misclassification of herbaceous wetlands, which cover a significant proportion of the land mass in Eurasian Arctic. Mosses (especially *Sphagnum* mosses) and lichens on herbaceous wetlands exhibit distinct spectral signatures and a seasonal pattern of change that is substantially different from other plants in the “herbaceous” group.

The analysis of land-cover maps at two test sites highlighted specific strengths and weaknesses of the examined land-cover products in these two locations. At the St. Petersburg site both categorical maps agreed well, but both exaggerated tree cover and under-reported shrub and herbaceous vegetation. At the Komi site, the over-reporting of tree cover by GLC-2000 and failure of MODIS.PFT to separate shrub and herbaceous vegetation were the major issues in representing the overall land cover. Depending on specific application of the map other features may be significant, such as under-reporting of small but abundant water bodies in the arctic region on categorical coarse-resolution maps.

Different vegetation maps used in biogeochemical modeling could produce substantially different estimates of the regional C balance. A simple analysis in which we extrapolated simulated C stock and flux density for dominant vegetation types across the area estimates of these types in different land-cover products showed that a very different picture of the regional C balance emerges when changing the ratio of tree cover (an estimated C source) to shrub cover (C sink). A separate examination of live vegetation C indicated that the use of GLC-2000 map could lead to substantially higher estimate of C stock in forest biomass and greater role of trees as C sink than MODIS.PFT map. While simplified calculations provide a

general idea of how the underlying vegetation data can change regional C balance estimates, a more detailed comparison of its effects would require additional, spatially-explicit simulations using each of the different land-cover maps to drive the model.

References

- Anisimov OA, Vaughan DG, Callaghan TV, Furgal C, Marchant H, Prowse TD, Vilhjálmsson H, Walsh JE (2007) Polar regions (Arctic and Antarctic) In: Parry ML, Canziani OF, Palutikof JP, van der Linden PJ, Hanson CE (eds) *Climate change 2007: impacts, adaptation and vulnerability, contribution of working group II to the fourth assessment report of the intergovernmental panel on climate change*. Cambridge University Press, Cambridge, pp 653–685
- Balshi MS, McGuire AD, Zhuang Q, Melillo J, Kicklighter DW, Kasischke E, Wirth C, Flannigan M, Harden J, Clein JS, Burnside TJ, McAllister J, Kurz WA, Apps M, Shvidenko A (2007) The role of historical fire disturbance in the carbon dynamics of the pan-boreal region: a process-based analysis. *J Geophys Res* 112. doi:10.1029/2006JG000380
- Bartalev SA, Belward AS, Erchov DV, Isaev AS (2003) A new Spot4-Vegetation Derived Land Cover Map of Northern Eurasia. *Int J Rem Sens* 24:1977–1982
- Bonan GB, Levis S, Kergoat L, Oleson KW (2002) Landscapes as patches of plant functional types: an integrating concept for climate and ecosystem models. *Glob Biogeochem Cycles* 16. doi:10.1029/2000GB001360
- Breiman L (1996) Bagging predictors. *Mach Learn* 26:123–140
- Bubier JL, Rock BN, Crill PM (1997) Spectral reflectance measurements of boreal wetland and forest mosses. *J Geophys Res-Atmos* 102:29483–29494
- Canty MJ, Nielsen AA, Schmidt M (2004) Automatic radiometric normalization of multispectral imagery. *Rem Sens Environ* 91:441–451
- Chapin FS III, Sturm M, Serreze MC, McFadden JP, Key JR, Lloyd AH, McGuire AD, Rupp TS, Lynch AH, Schimel JP, Beringer J, Chapman WL, Epstein HE, Euskirchen ES, Hinzman LD, Jia G, Ping CL, Tape KD, Thompson CDC, Walker DA, Welker JM (2005) Role of land-surface changes in Arctic summer warming. *Science* 310:657–660
- Chapin FS III, Woodwell GM, Randerson JT, Rastetter EB, Lovett GM, Baldocchi DD, Clark DA, Harmon ME, Schimel DS, Valentini R, Wirth C, Aber JD, Cole JJ, Goulden ML, Harden JW, Heimann M, Howarth RW, Matson PA, McGuire AD, Melillo JM, Mooney HA, Neff JC, Houghton RA, Pace ML, Ryan MG, Running SW, Sala OE, Schlesinger WH, Schulze ED (2006) Reconciling carbon-cycle concepts, terminology, and methods. *Ecosystems* 9:1041–1050. doi:10.1007/s10021-005-0105-7
- Chavez PS Jr (1996) Image-based atmospheric corrections – revisited and improved. *Photogramm Eng Rem Sens* 62:1025–1036
- Commission of the European Communities (1993) *CORINE land cover: guide technique*. Brussels, Belgium
- Crist EP (1985) A TM tasseled cap equivalent transformation for reflectance factor data. *Rem Sens Environ* 17:301–306
- DeFries RS, Townshend JRG (1994) NDVI derived land cover classifications at a global scale. *Int J Rem Sens* 15:3567–3586
- DeFries RS, Hansen M, Steininger M, Dubayah R, Sohlberg R, Townshend JRG (1997) Subpixel forest cover in central Africa from multisensor, multitemporal data. *Rem Sens Environ* 60:228–246
- Di Gregorio A (2005) *Land cover classification system: classification concepts and user manual for software – version 2*, Rome
- EUROSTAT (1998) *Forestry statistics 1992–1996*, Luxembourg
- Field CB, Lobell DB, Peters HA, Chiariello NR (2007) Feedbacks of terrestrial ecosystems to climate change. *Ann Rev Environ Res* 32:1–29

- Frey KE, Smith LC (2007) How well do we know northern land cover: Comparison of four global vegetation and wetland products with a new ground-truth database for West Siberia. *Glob Biogeochem Cycles* 21. doi:10.1029/2006GB002706
- Friedl MA, McIver DK, Hodges JCF, Zhang XY, Muchoney D, Strahler AH, Woodcock CE, Gopal S, Schneider A, Cooper A, Baccini A, Gao F, Schaaf CB (2002) Global land cover mapping from MODIS: algorithms and early results. *Rem Sens Environ* 83:287–302
- Fritz S, Bartholome E, Belward A, Hartley A, Stibig HJ, Eva H, Mayaux P, Bartalev SA, Latifovic R, Kolmert S, Roy PS, Agrawal S, Bingfan W, Wenting X, Ledwith M, Pekel JF, Giri C, Mucher S, de Badts E, Tateishi R, Champeaux JL, Defourny P (2003) Harmonisation, mosaicing and production of the Global Land Cover 2000 database, *Ispra*
- Fritz S, Lee L (2005). Comparison of land cover maps using fuzzy agreement. *Int J Geogr Inf Sci* 19:787–807
- Frohn RC, Hinkel KM, Eisner WR (2005) Satellite remote sensing classification of thaw lakes and drained thaw lake basins on the North Slope of Alaska. *Rem Sens Environ* 97:116–126
- Giri C, Zhu ZL, Reed B (2005) A comparative analysis of the Global Land Cover 2000 and MODIS land cover data sets. *Rem Sens Environ* 94:123–132
- Gurney KR, Scott Denning A, Rayner P, Pak B, Baker D, Bousquet P, Bruhwiler L, Chen YH, Ciais P, Fung IY, Heimann M, Higuchi K, John J, Maki T, Maksyutov S, Peylin P, Prather M, Taguchi S (2004) Transcom 3 inversion intercomparison: Model mean results for the estimation of seasonal carbon sources and sinks. *Glob Biogeochem Cycles* 18:GB1010. doi:10.1029/2003GB002111
- Häme T, Stenberg P, Rauste Y (2000) A methodology to estimate forest variables at sub-pixel level. In: Zawila-Niedzwiecki T, Brach M (eds) *Proceedings of conference on remote sensing and forest monitoring*, Rogow
- Häme T, Stenberg P, Andersson K, Rauste Y, Kennedy P, Folving S, Sarkeala J (2001) AVHRR-based forest proportion map of the Pan-European area. *Rem Sens Environ* 77:76–91
- Hansen MC, DeFries RS, Townshend JRG, Sohlberg R (2000) Global land cover classification at 1 km resolution using a decision tree classifier. *Int J Rem Sens* 21:1331–1365
- Hansen MC, DeFries RS, Townshend J, Sohlberg R, Carroll M, Dimiceli C (2002) Towards an operational MODIS continuous field of percent tree cover algorithm: examples using AVHRR and MODIS data. *Rem Sens Environ* 83(1–2):303–319
- Hansen MC, DeFries RS, Townshend JRG, Carroll M, Dimiceli C, Sohlberg RA (2003a) Global percent tree cover at a spatial resolution of 500 meters: First results of the MODIS vegetation continuous fields algorithm. *Earth Interact* 7:1–15
- Hansen MC, DeFries RS, Townshend JRG, Carroll M, Dimiceli C, Sohlberg R (2003b) *Vegetation continuous fields MOD44B, 2001 percent tree cover – collection 3*, College Park
- Hansen MC, Townshend JRG, DeFries RS, Carroll M (2005) Estimation of tree cover using MODIS data at global, continental and regional/local scales. *Int J Rem Sens* 26:4359–4380
- Hansen MC, Stehman SV, Potapov PV, Loveland TR, Townshend JRG, DeFries RS, Pittman KW, Stolle F, Steining MK, Carroll M, Dimiceli C (2010) Humid tropical forest clearing from 2000 to 2005 quantified using multi-temporal and multi-resolution remotely sensed data. *Proceedings of the national academy of sciences of USA* 107(19):8650–8655
- Heiskanen J (2008) Evaluation of global land cover data sets over the tundra-taiga transition zone in northernmost Finland. *Int J Rem Sens* 29:3727–3751
- Herold M, Mayaux P, Woodcock CE, Baccini A, Schmullius C (2008) Some challenges in global land cover mapping: An assessment of agreement and accuracy in existing 1 km datasets. *Rem Sens Environ* 112(5). doi:10.1016/j.rse.2007.11.013
- Houghton RA (2003) Why are estimates of the terrestrial carbon balance so different. *Glob Chang Biol* 9:500–509
- Houghton RA, Joos F, Asner GP (2004) The effects of land use and management on the global carbon cycle. In: Gutman G, Janetos AC, Justice CO, Moran EF, Mustard JF, Rindfuss RR, Skole D, Turner BL II, Cochrane MA (eds) *Land change science: Observing, monitoring, and understanding trajectories of change on the Earth's surface*. Kluwer Academic Publishers, Dordrecht

- Hurtt GC, Frohling S, Fearon MG, Moore B III, Shevliakova E, Malyshev S, Pacala S, Houghton RA (2006) The underpinnings of land-use history: Three centuries of global gridded land-use transitions, wood harvest activity, and resulting secondary lands. *Glob Chang Biol* 12:1–22
- Jung M, Henkel K, Herold M, Churkina G (2006) Exploiting synergies of global land cover products for carbon cycle modeling. *Rem Sens Environ* 101:534–553
- Kennedy RE, Cohen WB (2003) Automated designation of tie-points for image-to-image coregistration. *Int J Rem Sens* 24:3467–3490
- Krankina ON, Fiorella M, Cohen W, Treyfeld RF (1998) The use of Russian forest inventory data for carbon budgeting and for developing carbon offset strategies. *World Res Rev* 10:52–66
- Krankina ON, Houghton RA, Harmon ME, Hogg EH, Butman D, Yatskov M, Huso M, Treyfeld RF, Razuvaev VN, Spycher G (2005) Effects of climate and disturbance on forest biomass across Russia. *Can J For Res* 35:2281–2293
- Krankina ON, Pflugmacher D, Friedl M, Cohen WB, Nelson P, Baccini A (2008) Meeting the challenge of mapping peatlands with remotely sensed data. *Biogeosci Discuss* 5:1–26
- Kukuev YA, Krankina ON, Harmon ME (1997) The forest inventory system in Russia. *J Forest* 95:15–20
- Loveland TR, Reed BC, Brown JF, Ohlen DO, Zhu Z, Yang L, Merchant JW (2000) Development of a global land cover characteristics database and IGBP DISCover from 1 km AVHRR data. *Int J Rem Sens* 21:1303–1330
- Matthews E, Fung I (1987) Methane emission from natural wetlands: Global distribution, area, and environmental characteristics of sources. *Glob Biogeochem Cycles* 1:61–86
- McGuire AD, Melillo JM, Kicklighter DW, Pan Y, Xiao X, Helfrich J, Moore B III, Vorosmarty CJ, Schloss AL (1997) Equilibrium responses of global net primary production and carbon storage to doubled atmospheric carbon dioxide: Sensitivity to changes in vegetation nitrogen concentration. *Glob Biogeochem Cycles* 11:173–189
- McGuire AD, Chapin F S III, Wirth C, Apps M, Bhatti J, Callaghan T, Christensen T R, Clein J S, Fukuda M, Maximov T, Onuchin A, Shvidenko A, Vaganov E (2007) Responses of high latitude ecosystems to global change: Potential consequences for the climate system In: Canadell JG, Pataki DE, Pitelka LF (eds.) *Terrestrial Ecosystems in a Changing World*. The IGBP Series. Springer, Berlin, pp 297–310
- Mitchell TD, Jones PD (2005) An improved method of constructing a database of monthly climate observations and associated high-resolution grids. *Int J Climatol* 25(6):693–712
- Morissette JT, Privette JL, Justice CO (2002) A framework for the validation of MODIS Land products. *Rem Sens Environ* 83:77–96
- Myneni RB, Dong J, Tucker CJ, Kaufmann RK, Kauppi PE, Liski J, Zhou L, Alexeyev V, Hughes MK (2001) A large carbon sink in the woody biomass of northern forests. *Proc Natl Acad Sci of USA* 98:14784–14789
- Päivinen R, Lehtikoinen M, Schuck A, Häme T, Väättäinen S, Kennedy P, Folving S (2001) Combining earth observation data and forest statistics. European Forest Institute, Joint Research Centre – European Commission, EFI Research Report 14, Joensuu, Finland and Ispra
- Pflugmacher D, Krankina ON, Cohen WB (2007) Satellite-based peatland mapping: Potential of the MODIS sensor. *Glob Planet Change* 56:248–257
- Polyakov ID, Alekseev GV, Bekryaev RV, Bhatt U, Colony R, Johnson MA, Karklin VP, Makshtas AP, Walsh D Yulin AV (2002) Observationally based assessment of polar amplification of global warming. *Geophys Res Lett* 29. doi:10.1029/2001GL011111
- Potapov P, Hansen MC, Stehman SV, Loveland TR, Pittman K (2008) Combining MODIS and Landsat imagery to estimate and map boreal forest cover loss. *Rem Sens Environ* 112: 3708–3719
- Rahman H, Dedieu G (1994) SMAC: A simplified method for the atmospheric correction of satellite measurements in the solar spectrum. *Int J Rem Sens* 15:123–143
- Raich JW, Rastetter EB, Melillo JM, Kicklighter DW, Steudler DA, Peterson BJ, Grace AL, Moore B III, Vörösmarty CJ (1991) Potential net primary productivity in South America: Application of a global model. *Ecol Appl* 1:399–429

- Schimel DS, House JI, Hibbard KA, Bousquet P, Ciais P, Peylin P, Braswell BH, Apps MJ, Baker D, Bondeau A, Canadell J, Churkina G, Cramer W, Denning AS, Field CB, Friedlingstein P, Goodale C, Heimann M, Houghton RA, Melillo JM, Moore B III, Murdiyarso D, Noble I, Pacala SW, Prentice IC, Raupach MR, Rayner PJ, Scholes RJ, Steffen WL, Wirth C (2001) Recent patterns and mechanisms of carbon exchange by terrestrial ecosystems. *Nature* 414:169–172. doi:10.1038/35102500
- Schlesinger WH (1991) *Biogeochemistry: An analysis of global change*. San Diego, New York
- Schuck A, Van Brusselen J, Päivinen R, Häme T, Kennedy P, Folving S (2002) Compilation of a calibrated European forest map derived from NOAA-AVHRR data. European Forest Institute. EFI Internal Report 13, 44 pp plus Annexes
- Shvidenko A, Nilsson S (2003) A synthesis of the impact of Russian forests on the global carbon budget for 1961–1998. *Tellus* 55B:391–415
- Sukhinin AI, French NHF, Kasischke ES, Hewson JH, Soja AJ, Csiszar IA, Hyer EJ, Loboda T, Conrad SG, Romasko VI, Pavlichenko EA, Miskiv SI, Slinkina OA (2004) AVHRR-based mapping of fires in Russia: New products for fire management and carbon cycle studies. *Rem Sens Environ* 93(4):546–564
- Stahler AH, Boschetti L, Foody GM, Friedl MA, Hansen MC, Herold M, Mayaux P, Morisette JT, Stehman SV, Woodcock CE (2006) Global land cover validation: Recommendations for evaluation and accuracy assessment of global land cover maps. Luxembourg: Office for Official Publications of the European Communities, 60 pp
- Stroeve J, Markus T, Meier W, Miller J (2006) Recent changes in the Arctic melt season. *Ann Glaciol* 44(1):367–374. doi:10.3189/172756406781811583
- van der Werf GR, Randerson JT, Giglio L, Collatz GJ, Kasibhatla PS, Arellano Jr. AF (2006) Interannual variability in global biomass burning emissions from 1997 to 2004. *Atmos Chem Phys* 6:3423–3441
- Vogelmann JE, Moss DM (1993) Spectral reflectance measurements in the Genus Sphagnum. *Rem Sens Environ* 45:273–279
- Walker DA, Reynolds MK, Daniels FJA, Einarsson E, Elvebakk A, Gould WA, Katenin AE, Kholod SS, Markon CJ, Melnikov ES, Moskalenko NG, Talbot SS, Yurtsev BA, Team C. (2005) The circumpolar Arctic vegetation map. *J Veg Sci* 16:267–282
- Wan Z, Zhang Y, Zhang Q, Li ZL (2002) Validation of the land surface temperature products retrieved from Terra Moderate Resolution Imaging Spectroradiometer data. *Rem Sens Environ* 83:163–180
- Wolfe RE, Roy DP, Vermote EF (1998) MODIS land data storage, gridding, and compositing methodology: Level 2 grid. *IEEE Trans Geosci Rem Sens* 36(4):1324–1338
- Wu A, Li Z, Cihlar J (1995) Effects of land cover type and greenness on AVHRR bidirectional reflectances. *J Geophys Res* 100:9179–9192
- Zhu Z, Evans DL (1994) US forest types and predicted percent forest cover from AVHRR data. *Photogramm Eng Rem Sens* 60:525–531